

are shown in Table I as $\text{Ag}^0/\text{CD}_3\text{CN}$ (site I). The g factor of Ag^0 in site I is closer to the free-electron value,²⁵ and the silver isotropic hyperfine coupling in site I is closer to the free-atom value than in site II. Furthermore Ag^0 in site I seems to be a precursor to Ag^0 in site II since CNI converts to CNII on thermal annealing at 77 K. Also CNII can be converted back to CNI at 4 K by optical excitation with visible light. Since the signals are weak, the interconversion is only semiquantitative. This thermal/photo cyclic behavior is analogous to that found for Ag^0 in water matrices.²⁶

By analogy with the fairly complete ion/atom solvation picture obtained for Ag^0 in water matrices, we interpret Ag^+/Ag^0 solvation in CD_3CN matrices as follows. We suggest that Ag^+ is only weakly solvated by CD_3CN , which is expected from evidence that methyl cyanide generally solvates cations weakly.²⁷ Thus, we interpret that Ag^0 in CNI is characteristic of the Ag^+ solvation shell in CD_3CN . Indeed, since Ag^0 in CNI has the magnetic parameters of a nearly free silver atom, the solvation is quite weak. This is not the equilibrium solvation geometry for the atom however. Upon thermal excitation by warming above 50 K, Ag^0 converts from site CNI to CNII, which we interpret as an atom solvation process leading to a near equilibrium solvent environment for the atom. Geometrically we surmise that this atom solvation process has brought the four first solvation shell CD_3CN molecules closer to Ag^0 . This leads to some delocalization of the unpaired electron spin density from the Ag^0 to the solvent molecules. This decreases the Ag^0 isotropic coupling from 2006 to 1500 MHz and increases the N coupling on the solvent from unresolvable to a resolvable 16 MHz. In addition, the decreases in the g factor of Ag^0 indicate some admixture of other orbitals such as 5p into the unpaired electron wave function. We suggest that the delocalization causes the solvation shell of the atom to be more compact than that

of the ion. Thus, we have another example of a striking silver atom solvation effect. One might also interpret these changes as due to redistribution among different types of trapping sites. However, on the basis of our previous detailed studies in aqueous matrices, we believe the solvation description is best.

The reversal of atom solvation, which we will term desolvation, by optical excitation of site CNII at 4 K can only be understood qualitatively. We offer the same explanation advanced for the optically driven desolvation of Ag^0 in water matrices. Namely, the excited state has significant charge-transfer-to-solvent character such that the excited state looks more like a Ag^+ core to the nearest CN groups so they move toward a geometry consistent with this. And at 4 K they become locked into this resolved atom geometry.

It remains to comment on the low yield of Ag^0 in site CNII initially formed in the 4 K radiolysis. It seems probable that this is due to the most energetic secondary electrons produced by the radiation. These energetic electrons initially form Ag^0 in CNI, but the additional energy available converts CNI to CNII. The majority of the secondary electrons are trapped by the matrix. When these are thermally detrapped, they initially react with Ag^+ to produce Ag^0 in CNI, but site CNI is not observable because the thermal energy is sufficient to cause immediate conversion to site CNII.

It is also interesting to note that the magnetic parameters of Ag^0 in site CNI are similar to those of a site "2020" observed at 77 K in alcohol-water mixed matrices¹³ (see Table I). Likewise, a similar site has been seen in methyl cyanide-water mixed matrices at 77 K and termed species B.¹⁹ These sites in mixed matrices have been assigned to a mixed first solvation shell and to some sort of an interstitial site created by local disorder in the mixed matrix. To the extent that site CNI is indeed analogous, this interpretation of the 2020 site and species B may need to be reassessed.

Acknowledgment. This work was partially supported by the Department of Energy.

(25) Ramsey, N. F. In "Molecular Beams"; Clarendon Press: Oxford, 1955.

(26) Kevan, L. *J. Chem. Phys.* 1978, 69, 3444.

(27) Kuntz, I. D.; Cheng, C. J. *J. Am. Chem. Soc.* 1975, 97, 4852.

Infrared Spectra of the Isobutyl and Neopentyl Radicals. Characteristic Spectra of Primary, Secondary, and Tertiary Alkyl Radicals

J. Pacansky,* D. W. Brown, and J. S. Chang

IBM Research Laboratory, San Jose, California 95193 (Received: December 31, 1980; In Final Form: May 14, 1981)

Infrared spectra are presented for the isobutyl and neopentyl radicals for the first time. Significant differences are observed in the β -CH stretching and pyramidal bending regions between primary alkyl radicals with straight chains and those with branched chains like the isobutyl and neopentyl radicals. These are compared with spectra of other alkyl radicals to establish characteristic infrared spectra of primary, secondary, and tertiary alkyl radicals.

Introduction

Characteristic infrared spectra of organic materials are very important for identifying functional groups, and investigating structural changes a particular group exerts on the rest of a molecular system.^{1,2} In order to determine

characteristic spectra, we investigated a series of structurally related systems spectroscopically to establish a trend. Although this is not a trivial task, it is nevertheless somewhat easier for molecular systems with closed shells. The task is nontrivial and challenging for systems with

(1) L. J. Bellamy, "Advances in Infrared Group Frequencies", Methuen, London, 1968.

(2) C. N. Rao, "Chemical Applications of Infrared Spectroscopy", Academic Press, New York, 1963.

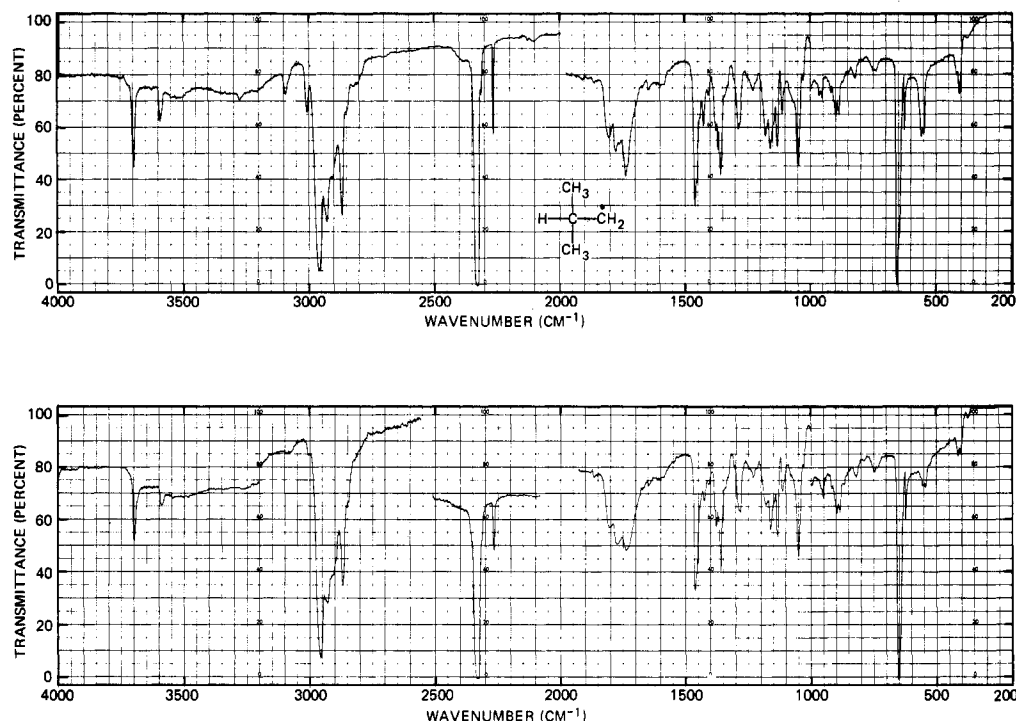


Figure 1. The infrared spectrum of the isobutyl radical and CO_2 (top) obtained by UV irradiation of the diacyl peroxide $((\text{CH}_3)_2\text{CHCH}_2\text{CO}_2\text{OCC-CH}_2\text{CH}(\text{CH}_3)_2)$ in an argon matrix at $T = 10$ K. The spectrum at the bottom was recorded after warming the matrix to $T = 38$ K and consists of the combination-disproportionation products of the isobutyl radical and CO_2 .

open shells, in particular those that have a very low or zero activation energy for combination and/or disproportionation. Since infrared spectra for open shells are not abundantly found in the literature, then establishing their characteristic vibrational spectra should provide new structural data and accelerate research on these systems.

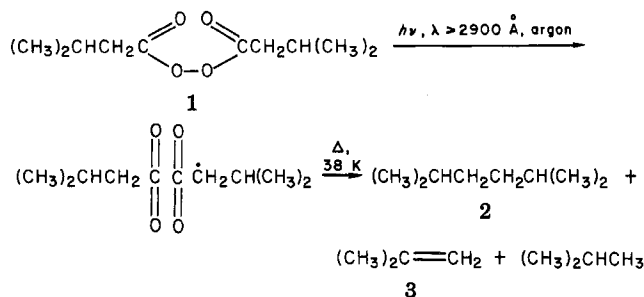
Earlier, we reported³ the characteristic infrared spectra of primary alkyl radicals where the length of the carbon chain was varied, e.g., the ethyl, *n*-propyl, and *n*-butyl radicals. Here, the infrared spectra of two additional primary alkyl radicals are reported—the isobutyl and neopentyl systems—in order to investigate the effect of increased branching of the hydrocarbon chain on the primary radical center. In addition, we show a comparison of the infrared spectra of primary alkyl radicals with secondary and tertiary radicals to develop the characteristic infrared spectra for hydrocarbons with primary, secondary, and tertiary radical centers.

Experimental Section

The diacyl peroxides were prepared by the method outlined by Johnson.⁴ This synthetic method, i.e., the preparation of diacyl peroxides by reaction of acid chlorides with potassium superoxide, gave peroxides which were more suitable for matrix isolation studies than the method outlined by Kochi.⁵ Diacyl peroxides are rather unstable materials and one should exercise due caution when handling these materials.

The infrared spectra were recorded on either a Perkin-Elmer 621 or Beckman IR-12 spectrometer. The cryogenic equipment and photochemical apparatus have been extensively described in other reports.^{3,6,7}

Scheme I



Results

The isobutyl radical was obtained by UV irradiation ($\lambda > 2900 \text{ \AA}$) of the diacyl peroxide (1) isolated in an argon matrix (concentration = 1/500) at $T = 10$ K. The infrared spectrum recorded after complete destruction of the peroxide to CO_2 and the radical is shown in Figure 1. The spectral features at 3115, 3023, 2820, and 555 cm^{-1} are assigned to the isobutyl radical on the basis that upon warmup of the argon matrix to 38 K a synchronous disappearance of the bands occurs with the appearance of the combination-disproportionation products (2, 3) of the isobutyl radical. The infrared spectrum recorded after the brief warmup of the matrix is also shown in Figure 1. These results are summarized in Scheme I.

The neopentyl radical was prepared in an identical manner. The infrared spectrum after complete conversion of the diacyl peroxide (4) to radical and CO_2 is shown in Figure 2. The spectrum which results after warming of the argon matrix to $T = 38$ K for a relatively extensive time ($t = 30$ min) is also shown in Figure 2. Normally, the radicals will react in times which vary from several seconds at $T \approx 38$ K to several minutes; the neopentyl radical required rather drastic measures probably because only

(3) J. Pacansky, D. E. Horne, G. P. Gardini, and J. Bargon, *J. Phys. Chem.*, **81**, 2149 (1977).

(4) R. A. Johnson, *Tetrahedron Lett.*, 331 (1976).

(5) R. A. Sheldon and J. K. Kochi, *J. Am. Chem. Soc.*, **97**, 6896 (1975).

(6) J. Pacansky and H. Coufal, *J. Chem. Phys.*, **71**, 2811 (1979).

(7) J. Pacansky and H. Coufal, *J. Chem. Phys.*, **72**, 3298 (1980).

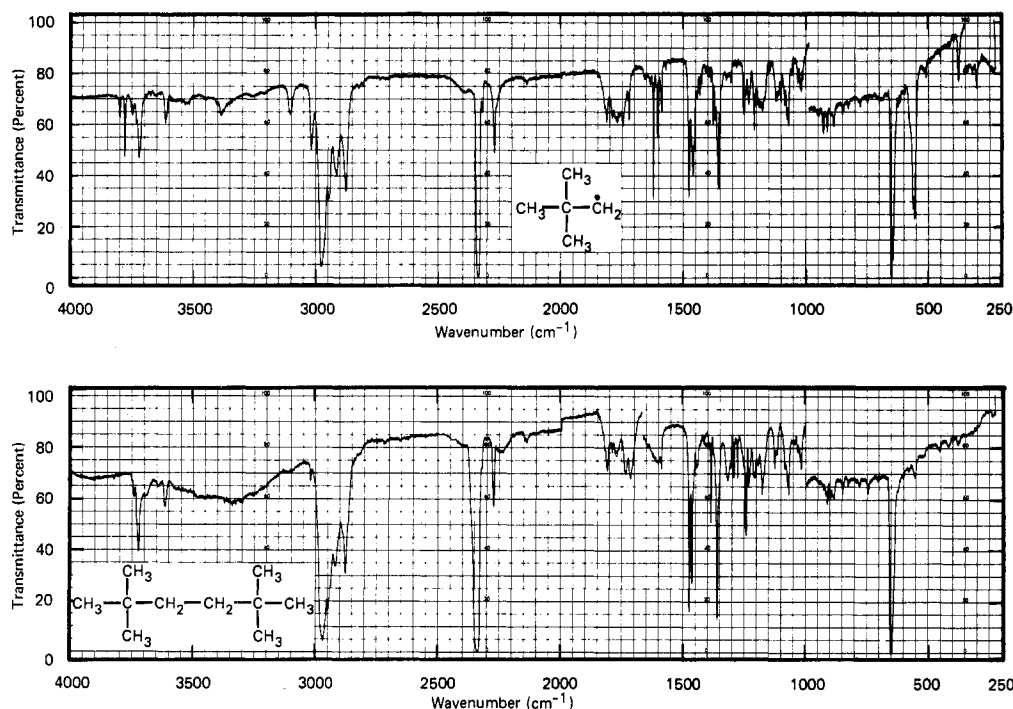
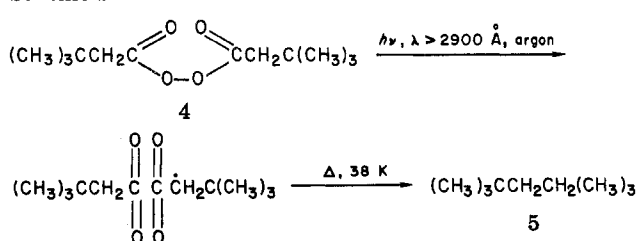


Figure 2. The infrared spectrum of the neopentyl radical and CO_2 (top) obtained by UV irradiation of the diacyl peroxide $((\text{CH}_3)_3\text{CCH}_2\text{CO}_2\text{O}_2\text{CC}-\text{H}_2\text{C}(\text{CH}_3)_3)$ in an argon matrix at $T = 10$ K. The spectrum at the bottom was recorded after warming the matrix to $T = 38$ K and consists of the combination product of the neopentyl radical.

TABLE I: Characteristic Infrared Absorptions (cm^{-1}) for Primary, Secondary, and Tertiary Alkyl Radicals

| | α -(CH) stretch | pyramidal bending | β -(CH) stretch |
|---|------------------------|---|----------------------------------|
| ethyl ($\text{CH}_3\dot{\text{C}}\text{H}_2$) | 3112.5, 3032.5 | 541.0 | 2840.0 |
| <i>n</i> -propyl ($\text{CH}_3\text{CH}_2\dot{\text{C}}\text{H}_2$) | 3100.0, 3017.5 | 530.0 | 2812.5 |
| <i>n</i> -butyl ($\text{CH}_3\text{CH}_2\text{CH}_2\dot{\text{C}}\text{H}_2$) | 3105.0, 3017.5 | 526.5 | 2800.0 |
| isobutyl ($(\text{CH}_3)_2\text{CH}\dot{\text{C}}\text{H}_2$) | 3115.0, 3023.0 | 557 } split 546 } 565 } 555 } | 2820.0 |
| neopentyl ($(\text{CH}_3)_3\text{C}\dot{\text{C}}\text{H}_2$) | 3105.0, 3020.0 | 382 } split 366 } <200 cm^{-1} | 2850 } split 2830 } 2825 } |
| isopropyl ($(\text{CH}_3)_2\dot{\text{C}}\text{H}$) | 3069 } split 3058 } | | |
| <i>tert</i> -butyl ($\dot{\text{C}}(\text{CH}_3)_3$) | | | |

Scheme II



the combination reaction occurred for this species. The infrared spectrum shown in Figure 2 certainly reflects this because bands due only to 2,5-dimethylhexane (5) are found. This is summarized in Scheme II.

Discussion

In general, the infrared spectrum of an alkyl radical consists of two parts, those modes which are a manifestation of the radical site and those which are quite similar to the spectra of the closed-shell parent hydrocarbon. In all the cases studied thus far, it could only be ascertained that the vibrational modes involving bonds α and β to the radical site are different from the spectra of hydrocarbons. Bonds more distant than this appear to be unaffected, and hence, the vibrational spectrum for this part of the alkyl radical appears to be quite similar to the spectrum of the

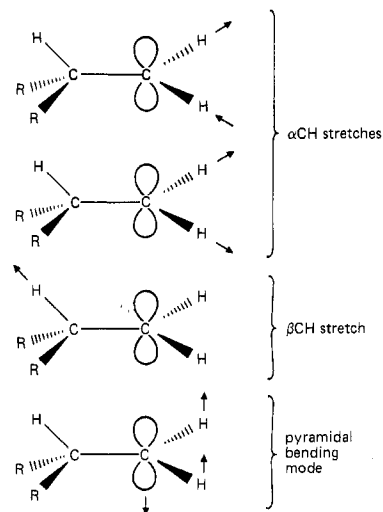


Figure 3. A pictorial illustration of the characteristic vibrational modes of primary alkyl radicals.

closed shell parent hydrocarbon. The specific vibrational modes involving the α and β bonds that are quite evident in the infrared spectra involve the pyramidal-like bending motion of the radical center, the symmetric and antisymmetric stretching of the α -CH bonds, and the stretching mode of the β -CH bonds. These are pictorially illustrated

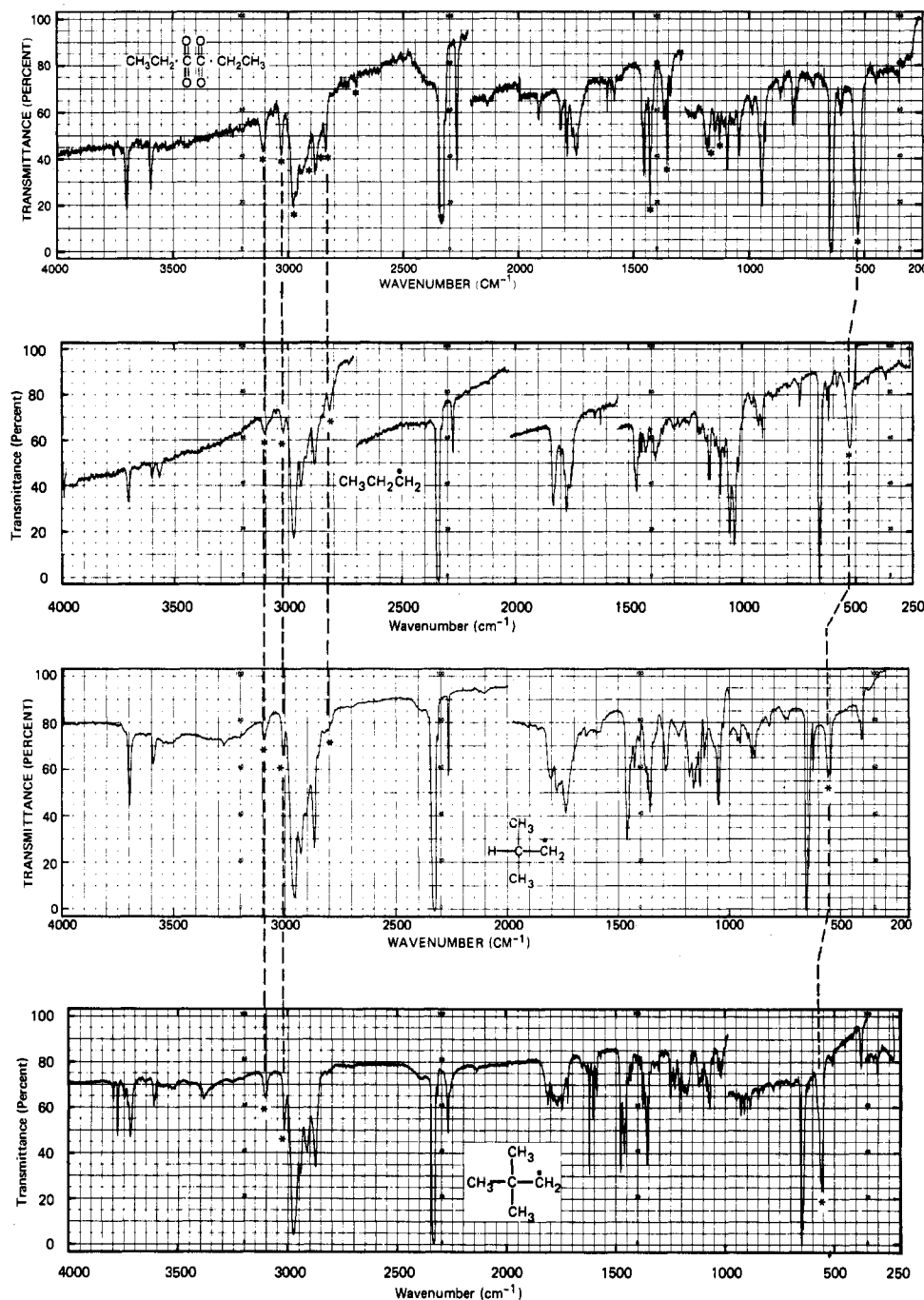


Figure 4. A comparison of the infrared spectra of primary alkyl radicals with straight chains ($\text{CH}_3\text{CH}_2\cdot$, $\text{CH}_3\text{CH}_2\text{CH}_2\cdot$) and branched chains ($(\text{CH}_3)_2\text{CHCH}_2\cdot$, $(\text{CH}_3)_3\text{CCH}_2\cdot$). The characteristic features for the radicals are connected by dashed lines in order to compare differences between the spectra.

in Figure 3 while Table I lists the observed band centers for the vibrations.

In Figure 4 the infrared spectra of the ethyl, *n*-propyl, isobutyl, and neopentyl radicals are shown in order to point out the important differences in the characteristic vibrational spectra of primary alkyl radicals as the branching of the hydrocarbon chain increases. The characteristic vibrational modes in each spectrum are connected by dotted lines to clearly distinguish them from other spectral features not pertinent for this discussion. The α -CH stretching frequencies centered at about 3110 and 3020 cm^{-1} change little from the ethyl to neopentyl radical. This is clearly shown in Figure 4 and listed in Table I. The β -CH stretching frequencies for the series shown in Figure 4, however, are more interesting. For example, while the frequencies and intensities are about the same for the ethyl and *n*-propyl radicals, a very broad absorption is observed

for the isobutyl radical, and none for neopentyl system. The latter is a trivial expectation since the neopentyl radical does not contain a β -CH bond. The broad absorption observed for the isobutyl radical may have its origin from two possible sources. Recent ab-initio calculations⁸ on the isobutyl radical indicate that two conformations are possible; the one lowest in energy has a β -CH bond eclipsed with the C_p orbital on the radical center while the other has a β -CC eclipsed and a β -CH bond almost perpendicular to the radical site. Since a barrier of only 0.17 kcal/mol separates the two conformations, then the broad absorption for the β -CH bond may be due to two different β -CH stretching frequencies which are not resolved in the spectrum shown in Figure 4 or, most likely,

(8) J. Pacansky and W. Schubert, *J. Am. Chem. Soc.*, submitted for publication.

due to a broadening created by a rapid interchange between the two nonequivalent β -CH bonds. A broadening due to a rapid rotation about the α -CC bond is more likely because at the temperature which the spectra were recorded ($T \approx 10$ K) the Arrhenius equation predicts (using a 0.17 kcal barrier) that the rate of interconversion between the two conformations of the isobutyl radical is competitive with the time required for a vibration.

The origin of the rather low frequency associated with the stretching of the β -CH bond is rather interesting because it is not observed in the infrared spectra of alkanes or alkenes.⁹ The absence of this feature in the infrared spectrum of the neopentyl radical, where no β -CH bonds are present, firmly establishes that a β -CH bond must be present for this absorption. Furthermore, experiments reported on the CH_3CH_2 and CHD_2CD_2 radicals¹⁰ reveal the nature of this vibrational mode. The low-frequency CH stretch observed at 2840 cm^{-1} for CH_3CH_2 may be due to a Fermi resonance between an overtone of the methyl internal deformation mode and a methyl CH stretching frequency.¹ This does not appear to be the case for alkyl radicals because the CH stretching frequency for the CHD_2CD_2 system, where the possibility of a vibrational resonance is eliminated, is almost coincident with the frequency observed for this mode in CH_3CH_2 . The low-frequency CH stretch observed for the CHD_2CD_2 radical reveals an important feature for β -CH bonds in alkyl radicals in general. McKean¹¹ has correlated vibrational frequencies with bond strengths for isolated CH bonds (e.g., in CHD_2CD_2). They have found that, in general, the observed vibrational frequency shifts to a lower value as the bond energy decreases. As a consequence of the studies of McKean and co-workers,¹¹ and the observations reported here for alkyl radicals in general, the infrared absorption observed in the low-frequency CH stretching region is assigned to a weak β -CH bond. This is supported by both thermodynamic and kinetic studies¹² on free radicals. In addition, extensive ab-initio calculations for the structure¹³ and vibrational frequencies¹⁴ of alkyl radicals have shown that the low-frequency β -CH stretches are a manifestation of longer than normal CH bonds.

The pyramidal bending mode for the primary radical center shifts from about 540 cm^{-1} for ethyl and *n*-propyl to slightly higher frequencies $\approx 560\text{ cm}^{-1}$ for the systems with more branching of the hydrocarbon chain. This is shown in Figure 4 and listed in Table I. The most important trend here is that the absorption for the isobutyl and neopentyl systems are split. This may be due to higher barriers for internal rotation compared to the ethyl and *n*-propyl radicals because in the isobutyl and neopentyl systems, isopropyl and tertiary butyl groups are rotated about the α -CC bond against the primary radical center. However, since the pyramidal bending motion should be coupled with the rotation about the α -CC bond to produce a complicated motion, then the splitting may have other origins than a higher barrier. A more complete account is forthcoming.

The spectra shown in Figures 4 and 5 contain sufficient information to establish the differences in vibrational spectra when an open shell is located at a number of different sites on a carbon chain. In essence, the spectra

represent the changes induced by substituting the hydrogens in the methyl radical with CH_3 groups and the β hydrogens in the ethyl radical with CH_3 groups. Since the spectra which result by CH_3 substitution of the β hydrogens in the ethyl radical have already been discussed, only the spectra created by α hydrogen substitution in the methyl radical are mentioned.

The infrared spectrum of the methyl radical¹⁵ consists of several very weak features and one extremely intense band attributed to the out-of-plane bending mode at 607 cm^{-1} . Substitution of one α hydrogen with a methyl group produces the ethyl radical whose more interesting spectrum, shown in Figure 5, has been noted above. The pyramidal bending mode observed at 607 cm^{-1} for the methyl radical is found at 540 cm^{-1} for the ethyl radical.

Substitution of a methyl group for an α hydrogen on the ethyl radical produces the isopropyl radical⁷ whose infrared spectrum characteristic for the α -CH stretching, β -CH stretching, and pyramidal bending modes are connected by dashed lines to those for the ethyl radical in Figure 5. In this case, the two high-frequency CH stretches at 3112.5 and 3032.5 cm^{-1} for the ethyl radical are replaced by one CH stretching at $\approx 3064\text{ cm}^{-1}$, characteristic of the single α -CH bond of the secondary radical site. The pyramidal bending frequency observed for the primary radical site at 540 cm^{-1} (ethyl radical) shifts to a significantly lower frequency, 369 cm^{-1} , for the secondary radical. The infrared absorption characteristic for the β -CH bonds is quite evident in the infrared spectrum of the isopropyl radical and is observed at 2840 cm^{-1} .

Exhaustive substitution of α hydrogens with methyl groups produces the tertiary butyl radical¹⁶ whose infrared spectrum is shown in Figure 5. There it is shown that neither α -CH bond stretches nor pyramidal bending modes are observed. The former is a trivial expectation but nevertheless supports the assignments for the CH stretching modes of the α -CH bonds for the primary and secondary radicals. The pyramidal bending frequency for the *tert*-butyl radical was not observed down to 200 cm^{-1} . A very important feature that remains in the spectrum of the *tert*-butyl radical is the band at 2825 cm^{-1} , characteristic of the stretching frequency for the β -CH bonds. It is particularly interesting to note that this is now the most intense band in the spectrum which is undoubtedly due to the presence of the three methyl groups about the radical center.

The trend in the absorptions for primary, secondary, and tertiary alkyl radicals are listed in Table I. Primary radical centers, i.e., radical sites located at the end of a hydrocarbon chain, are characterized by two olefinic-like α -CH stretches located at about $3100\text{--}3000\text{ cm}^{-1}$, and a broad intense absorption associated with the pyramidal bending mode between 540 and 500 cm^{-1} . Secondary radical centers, i.e., radical sites located within a hydrocarbon chain are characterized by one olefinic-like α -CH stretch located at about 3050 cm^{-1} and a much weaker absorption associated with the pyramidal bending mode at about 370 cm^{-1} . Tertiary radical centers are characterized by an intense band associated with the β -CH bonds. The frequency for the pyramidal bending mode is probably too low to be used as an aid in the identification of a tertiary radical site. In general, the number of CH stretching frequencies associated with the α -CH bonds together with the intensity and band center of the pyramidal bending mode may be used

(9) Similar low-frequency absorptions are observed for methyl groups substituted α to a heteroatom.

(10) J. Pacansky and H. Coufal, *J. Chem. Phys.*, **72**, 5285 (1980).

(11) D. C. McKean, *Chem. Soc. Rev.*, **7**, 399 (1978).

(12) J. A. Kerr, *Chem. Rev.*, **66**, 465 (1966).

(13) J. Pacansky and H. Dupuis, *J. Chem. Phys.*, **68**, 4276 (1978); **71**, 2095 (1979).

(14) M. Yoshimine and J. Pacansky, *J. Chem. Phys.*, **74**, 5168 (1981).

(15) D. E. Milligan and M. E. Jacox, *J. Chem. Phys.*, **47**, 5146 (1967); A. Snelson, *J. Phys. Chem.*, **75**, 537 (1970); J. Pacansky and J. Bargon, *J. Am. Chem. Soc.*, **97**, 6896 (1975).

(16) J. Pacansky and J. Chang, *J. Chem. Phys.*, **74**, 5539 (1981).

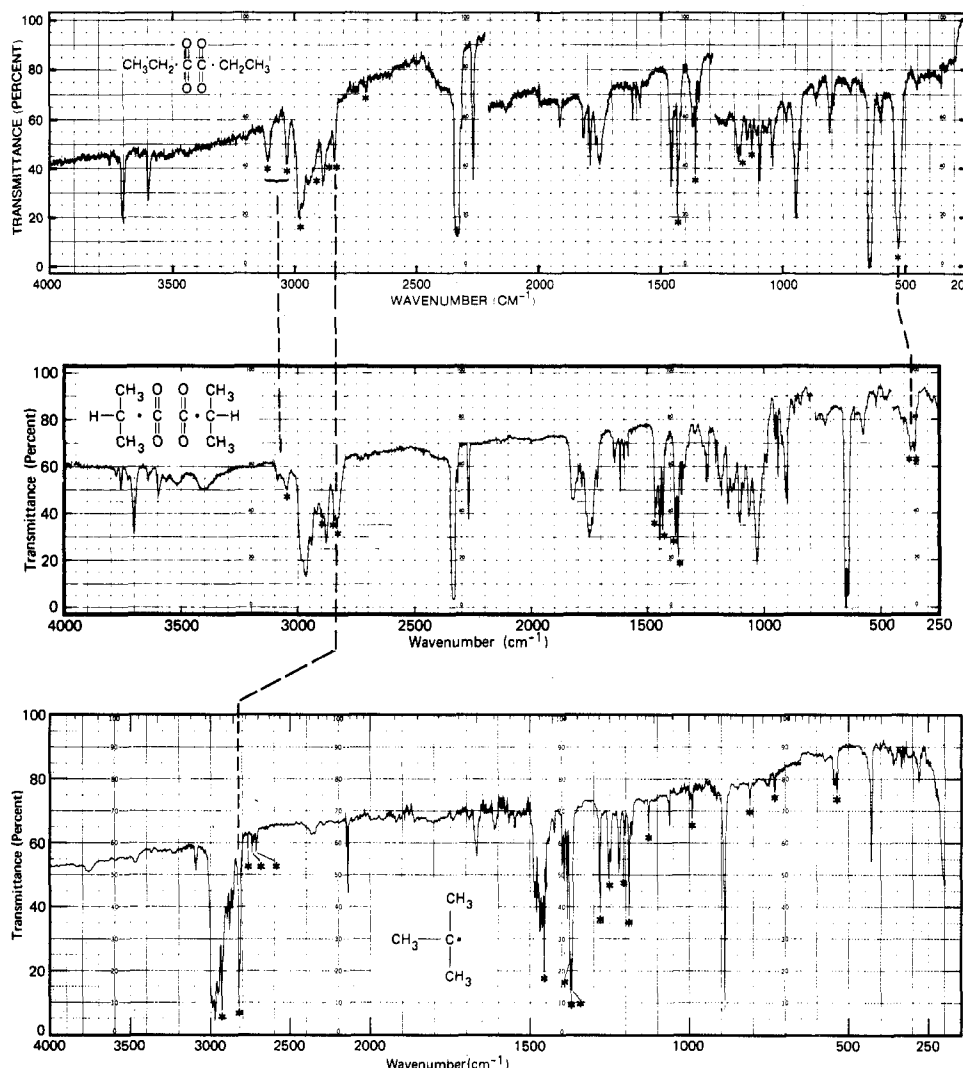


Figure 5. A comparison between the infrared spectra of ethyl, isopropyl, and *tert*-butyl radical to demonstrate the changes in infrared spectra between primary, secondary, and tertiary alkyl radicals.

to distinguish between primary and secondary radical centers.

Summary

Infrared spectra for the isobutyl and neopentyl radicals isolated in an argon matrix are shown for the first time.

The spectrum for the isobutyl radical indicates that rapid rotation takes place about the α -CC bond. The spectrum for the neopentyl radical clearly reveals that a β -CH bond must be present to obtain the abnormally low-frequency band observed for alkyl radicals in the CH stretching region.

Kinetics of the Reaction between Hydroxylamine and Sodium Bisulfite

S. Gomiscek,[†] R. Clem, T. Novakov, and S. G. Chang*

Lawrence Berkeley Laboratory, University of California, Berkeley, California 94720 (Received: January 13, 1981;
In Final Form: May 14, 1981)

Hydroxylamine and sulfur dioxide react in aqueous solution to form either sulfamic acid or ammonium bisulfate. Rate studies have been performed as a function of temperature. The rate law has been determined. The enthalpy and entropy of activation for the formation of both sulfamic acid and ammonium bisulfate have been evaluated.

Introduction

Sisler and Audrieth¹ studied the formation of sulfamic acid by the reaction of hydroxylamine with sulfur dioxide

in an aqueous solution and proposed that the reaction mechanism involved coordination between NH_2OH and SO_2 molecules with subsequent rearrangement to sulfamic

[†] On leave from the University of Ljubljana, Yugoslavia.

(1) H. H. Sisler and L. F. Audrieth, *J. Am. Chem. Soc.*, **61**, 3389 (1939).